Kinetic and Theoretical Studies on the Mechanism of Alkaline Hydrolysis of DNA

Naoya Takeda, Masahiko Shibata,† Nobuo Tajima,† Kimihiko Hirao,† and Makoto Komiyama*

Research Center for Advanced Science and Technology, The University of Tokyo, Komaba, Tokyo 153-8904, Japan, and Department of Applied Chemistry, Graduate School of Engineering, The University of Tokyo, Hongo, Tokyo 113-8656, Japan

Received March 7, 2000

The reaction mechanism of alkaline hydrolysis of DNA has been investigated by kinetic analysis and density-functional-theory calculation. The rates of hydrolysis of thymidine 3′-monophosphate esters (including thymidylyl(3′-5′)thymidine (Tp-OT)) monotonically decrease as the leaving groups get poorer. According to the theoretical calculation in which the solvent effects are incorporated, no intermediate is formed in the course of the reaction. In the alkaline hydrolysis of the activated Tp-OT analogues having good leaving groups, the 3′,5′-cyclic monophosphate of thymidine is concurrently formed through the intramolecular attack by the 5′-alkoxide ion. In the hydrolysis of the native dinucleotide, however, this side reaction does not occur, since the transition state leading to the departure of its poor leaving group cannot be formed due to conformational restraint. These arguments are supported by the theoretical analysis on the hydrolysis of both dimethyl phosphate and its O(bridging)→S substituted analogue.

Introduction

Nonenzymatic hydrolysis of DNA and RNA is one of the most important and attractive themes in nucleic acid chemistry. So far, many studies on the mechanism of RNA hydrolysis have been achieved.[1−4] A number of kinetic data have been accumulated and sufficiently rationalized by theoretical studies. However, the information on the mechanism of DNA hydrolysis has been scarce, mainly because spontaneous hydrolysis of DNA is virtually nil under physiological conditions. Recently, outstanding activities of lanthanide ions and other metal ions were found, and DNA was hydrolyzed at reasonable rates.[5−9] A new era has been opened in this field. The information on the mechanism of DNA hydrolysis[10,11] is crucially important for precise understanding of the catalytic mechanisms and also for design of active catalysts.

DNA hydrolysis consists of two stages (Figure 1). In the first stage, hydroxide ion attacks the phosphorus atom, and a pentacoordinated intermediate (or transition state) is formed. In the following stage, the bond between the P atom and the 5′-O (or 3′-O) atom of 2′-deoxyribonucleotide is cleaved. A pioneering quantum-chemical study on alkaline hydrolysis of dimethyl phosphate was achieved by Karplus et al.[12,13] However, correlation of the results with kinetic results has not been attempted.

In the present paper, both kinetic and theoretical approaches are adopted to investigate the mechanism of alkaline hydrolysis of DNA. Thymidylyl(3′-5′)thymidine (Tp-OT) and its analogues containing various leaving groups are hydrolyzed under alkaline conditions, and the dependence of hydrolysis rate on the basicity of leaving group is determined. The rates of intramolecular transesterification in these analogues, in which the P atom is attacked by the 5′-OH, are compared with the rates of alkaline hydrolysis. Theoretical studies are also achieved in the density-functional-theory calculation and the effect of substitution of the bridging O atom to an S atom is analyzed in detail. The structure of the transition-state is clarified, showing how it resembles the reactants or the products.

Results and Discussion

Alkaline Hydrolysis of Tp-OT and Its Analogues. (1) Kinetic Studies. At pH 14 and 80 °C, the pseudo-first-order rate-constant for alkaline hydrolysis (k_{hyd}) of Tp-OT is 2.0×10^{-3} h^{-1}. The products are thymidine (Thd) and its 3′- or 5′-monophosphate (Tp and pT, respectively), as expected.

To shed light on the reaction mechanism, the leaving group in Tp-OT was systematically changed, with the Tp moiety in the 5′-side kept constant (see Figure 2). The rate constants (k_{hyd}) for their hydrolyses are listed in

* To whom correspondence should be addressed. Tel and Fax: +81-3-5452-5209. E-mail: komiyama@mkomi.rcast.u-tokyo.ac.jp.
† Graduate School of Engineering.

(1) Perreault, D. M.; Anslyn, E. V. *Angew. Chem., Int. Ed. Engl.* **1997**, *36*, 432−450.
(2) Oivanen, M.; Kuusela, S.; Lönnberg, H. *Chem. Rev.* **1998**, *98*, 961−990.
(3) Zhou, D.-M.; Taira, K. *Chem. Rev.* **1998**, *98*, 991−1026.
(4) Li, Y.; Breaker, R. R. *J. Am. Chem. Soc.* **1999**, *121*, 5364−5372.
(5) Shiiba, T.; Yonezawa, K.; Takeda, N.; Matsumoto, Y.; Yashiro, M.; Komiyama, M. *J. Mol. Catal.* **1993**, *84*, L21-L25.
(6) Takasaki, B. K.; Chin, J. *J. Am. Chem. Soc.* **1994**, *116*, 1121−1122.
(7) Komiyama, M.; Takeda, N.; Takahashi, Y.; Uchida, H.; Shiiba, T.; Kodama, T.; Yashiro, M. *J. Chem. Soc., Perkin Trans. 2* **1995**, 269−274.
(8) Irisawa, M.; Komiyama, M. *J. Biochem.* **1995**, *117*, 465−466.
(9) Takeda, N.; Imai, T.; Irisawa, M.; Sumaoka, J.; Yashiro, M.; Shigekawa, H.; Komiyama, M. *Chem. Lett.* **1996**, 599−600.
(10) Sumaoka, J.; Takeda, N.; Okada, Y.; Takahashi, H.; Shigekawa, H.; Komiyama, M. *Nucleic Acids Res. Symp. Ser.* **1998**, *39*, 137−138.
(11) The mechanism of Ce(IV) catalysis has been recently discussed. Komiyama, M.; Takeda, N.; Shigekawa, H. *J. Chem. Soc., Chem. Commun.* **1999**, 1443−1451.
(12) Dejaegere, A.; Lim, C.; Karplus, M. *J. Am. Chem. Soc.* **1991**, *113*, 4353−4355.
(13) Dejaegere, A.; Liang, X.; Karplus, M. *J. Chem. Soc., Faraday Trans.* **1994**, *90*, 1763−1770.

10.1021/jo000323d CCC: $19.00
Published on Web 06/21/2000

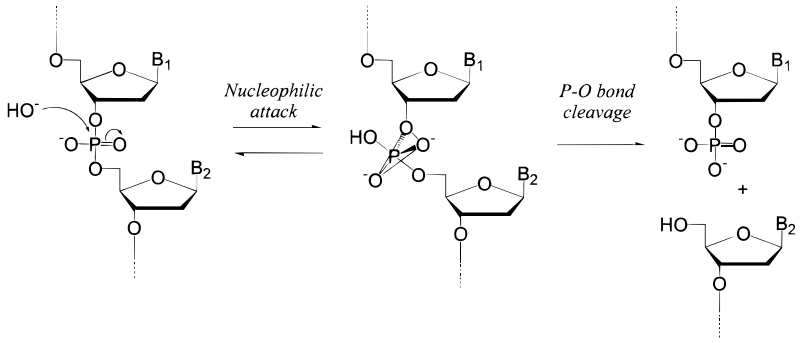

Figure 1. Scheme of DNA hydrolysis.

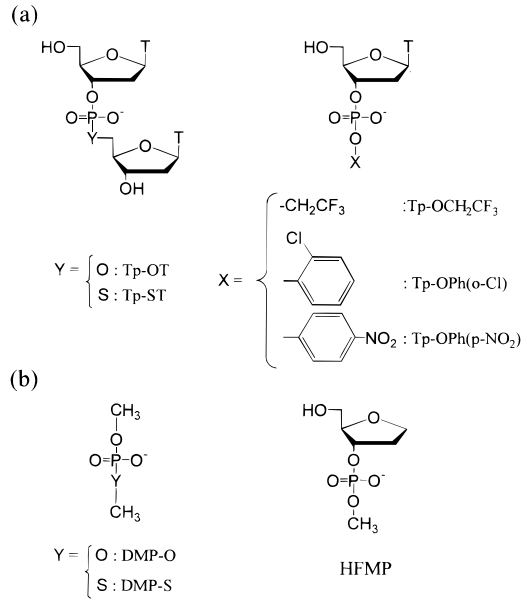

Figure 2. Structures of the substrates utilized in the present kinetic studies (a) and in the theoretical analyses (b).

Table 1. Pseudo-First-Order Rate Constants for the Alkaline Hydrolysis of Phosphodiester Linkage (k_{hyd}) and for the Intramolecular Transesterification by the 5′-OH Attack (k_{intra}) at pH 14 and 80 °C[a]

substrate	p$K_{a,lg}$[b]	k_{hyd}/h^{-1}	k_{intra}/h^{-1}
Tp-OT	14.8	2.0×10^{-3}	0[c]
Tp-OCH_2CF_3	12.4	3×10^{-3}[d]	2×10^{-3}[d]
Tp-ST	10.6	2.3×10^{-2}	6.6×10^{-2}
Tp-OPh(*o*-Cl)	8.1	4.2×10^{-2}	4.2×10^{-2}
Tp-OPh(*p*-NO_2)	7.2	3.2×10^{-1}	4.8×10^{-1}
Tp-(S)T	14.8	2.3×10^{-3}	
cTMP		1.2×10^{-1}	

[a] The error in the rate constants is around 10%, unless noted otherwise. [b] The pK_a values of the conjugate acids of the leaving groups.[14] [c] No cTMP was detected by the HPLC (see the ref 24). [d] Precise determination of the k_{hyd} and k_{intra} values is difficult, since the reaction is very slow (the error is around 30%).

Table 1 (these values were determined by using eqs 1 and 2, as described in the Experimental Section). When the bridging O atom in Tp-OT was replaced with S (Tp-ST), the hydrolysis rate increased by 11-fold ($k_{hyd} = 2.3 \times 10^{-2}$ h^{-1}). In contrast, Tp-(S)T, in which one of the two nonbridging O atoms in Tp-OT is substituted with S, was hydrolyzed at almost the same rate as Tp-OT. Apparently, the O→S substitution around the P atom does not significantly alter the electrophilicity of the P atom. Tp-ST is hydrolyzed faster than Tp-OT, since its leaving group is better; the pK_a's of R-SH and R-OH, the conjugate acids of leaving groups, (p$K_{a,lg}$) are around 10.6 and 14.8.[14] This argument is strongly supported by the fact that Tp-OCH_2CF_3 was hydrolyzed slightly faster than was Tp-OT, as expected from its smaller p$K_{a,lg}$ value (Table 1). Here, the perturbation around the P atom is marginal. The analogues involving aryl leaving groups were also hydrolyzed more promptly than Tp-OT.

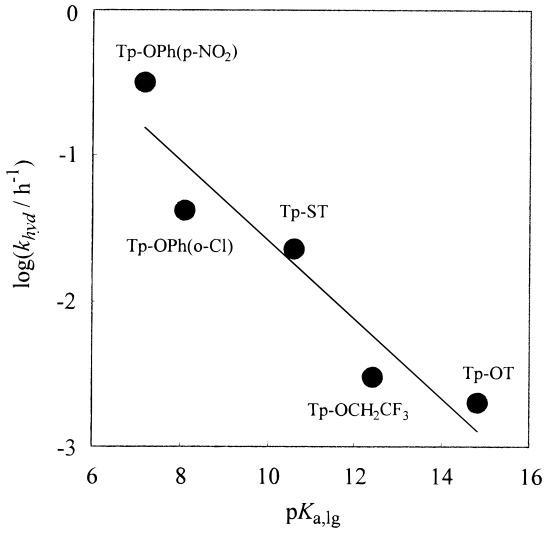

Figure 3. Brønsted-type correlation for the alkaline hydrolysis of Tp-OT and its analogues at pH 14 and 80 °C. All the data are from Table 1. The slope of the fitting line is −0.27.

As shown in Figure 3, the reaction rate monotonically decreases with increasing p$K_{a,lg}$: Tp-OPh(*p*-NO_2) > Tp-OPh(*o*-Cl) > Tp-ST > Tp-OCH_2CF_3 > Tp-OT. The removal of the leaving group from the P atom is, at least partially, rate limiting. The slope of this Brønsted-type plot is −0.27. This value is considerably smaller than the value (−0.76) reported by Chin et al.[15] This is probably because, in the present study, the esters of Tp were used as the substrates, to minimize undesirable perturbation

(14) pK_a values. (a) Tp-OT; its pK_a was taken as identical with the value of $CH_3OCH_2CH_2OH$ (Thompson, J. E.; Raines, R. T. *J. Am. Chem. Soc.* **1994**, *116*, 5467−5468; Ballinger, P.; Long, F. A. *J. Am. Chem. Soc.* **1960**, *82*, 795−798). (b) Tp-OCH_2CF_3 (Murto, J. *The Chemistry of Functional Groups, The Chemistry of the Hydroxyl Group, Part 2*; Patai, S., Ed; John Wiley & Sons: London, 1971; pp 1087−1115). (c) Tp-ST; estimated from the value of ethyl mercaptan (*Kagaku-binran Kisohen*; The Chemical Society of Japan, Ed.; Maruzen: Tokyo, 1984; II-339). (d) Tp-OPh(*o*-Cl) and Tp-OPh(*p*-NO_2) (Kortüm, G.; Vogel, W.; Andrussow, K. *Dissociation Constants of Organic Acids in Aqueous Solution*; Butterworth: London, 1961; pp 444−451). (e) H_2O (Sillén, L. G.; Martell, A. E. *Stability Constants of Metal-Ion Complexes, Supplement No 1*; The Chemical Society: London, 1971; pp 14−15).

(15) Chin, J.; Banaszczyk, M.; Jubian, V.; Zou, X. *J. Am. Chem. Soc.* **1989**, *111*, 186−190.

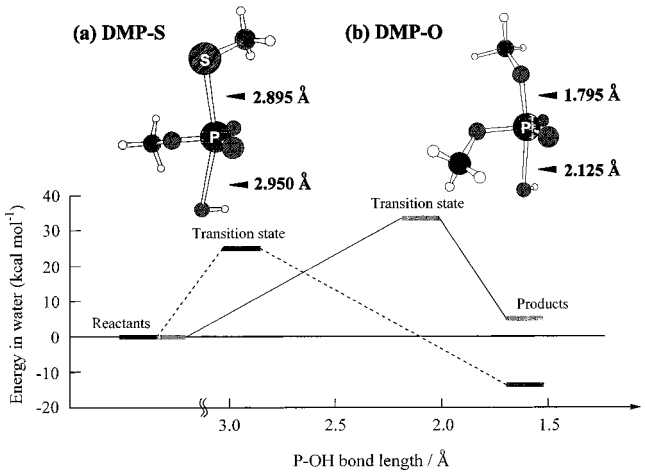

Figure 4. Energy-diagrams for the alkaline hydrolysis of DMP-O (the solid line) and DMP-S (the broken line). At the top, the structures of the transition states, optimized at RHF/6-31+G* level, are presented. The calculation was made at the B3LYP/6-31+G*//RHF/6-31+G* level, where the solvation effects were incorporated by the PCM method. The sum of the energy potentials of the reactants was taken as 0 kcal mol^{-1}.

around the P atom. In ref 15, the substrates were diaryl phosphates and dialkyl phosphates.

(2) Quantum-Chemical Studies. In the ab initio calculation, dimethyl phosphate (DMP-O) was used as a model compound of DNA. By using the polarized continuum model (PCM), the solvation effects by water molecules were sufficiently incorporated in the calculation of the Gibbs free energies. The charge of each atom in various species on the reaction-coordinate was evaluated by the natural population analysis. To examine the extents of the bond formation [P←O(attacking)] and the bond cleavage [P- - -O(leaving)] in the transition state, the imaginary frequencies were calculated by normal coordinate analysis of force constants. On optimizing the structures of phosphoranes, the calculations were started by placing a hydroxide ion and one of the OCH_3 groups in the DMP-O at the axial positions of the pentacoordinated P atom. The phosphoranes, formed from $(CH_3O)_2P(=O)(O^-)$ and OH^-, are dianionic (the two OH residues at the equatorial positions are dissociated), consistently with the corresponding pK_a values ($pK_{a1} = 6.5-11$ and $pK_{a2} = 11.3-15$).[1,16,17] The leaving OCH_3 group from the axial position departed as an anion.

According to this calculation, the alkaline hydrolysis proceeds in one step (the solid line in Figure 4). The activation free energy is 33.64 kcal mol^{-1}. No stable intermediate is formed along the reaction coordinate. In the transition state, the bond length between the O atom of the attacking OH residue (in the axial position) and the P atom is 2.125 Å. This bond is considerably longer than the bond (1.795 Å) between the O atom of the leaving OCH_3 and the P atom. The P−OH bond in the product ($CH_3OP(=O)(OH)(O^-)$) is 1.627 Å. In the transition state, the P−OH(axial) bond is partially formed, and the P−OCH_3(axial) bond is being kept still rather intact. Consistently, the imaginary frequency of P−OH(axial) bond (0.87564) is larger than that of the P−OCH_3(axial) bond (0.17324). The incomplete formation of this bond is further substantiated.

All these arguments were supported by the natural population analysis, in which the charge of each atom (i.e., atomic charge) is accurately evaluated.[18] The charges for the O atoms of OH^- (nucleophile) and of the OH residue in the product ($CH_3OP(=O)(OH)(O^-)$) are −1.47 and −1.08, respectively. The corresponding value of the O atom of the P−OH(axial) group in the transition state is −1.25. According to the Leffler's approach,[19] the extent of the formation of the P−OH bond in the transition state (α) is estimated to be 56.5% (= [−1.47 − (−1.25)]/[−1.47 − (−1.08)]). Similarly, the extent of the P−OCH_3 bond cleavage in the transition state (β) is estimated as 14.2% (the charges of the O atoms of the leaving OCH_3 group in DMP-O, of the P−OCH_3(axial) in the transition state and of the product (CH_3O^-) are −0.89, −0.92, and −1.13, respectively). The transition state resembles the initial state, rather than the products (vide post).[20] These results fairly agree with the structural analysis using P−O bond length (described above) and also with the small slope (−0.27) in the Brønsted-type plot in Figure 3.

When the quantum-chemical calculation was made on the DMP-O hydrolysis *in a gas phase* (without the contribution of the solvent effects), the energy barrier for the second stage (relating to the scission of the P−OCH_3 linkage) was increased, and an intermediate emerged between the two transition states (the OH^- attack and the P−OCH_3 scission). However, the former energy barrier is higher than the latter by only 0.99 kcal mol^{-1} and the energy-well is too shallow to be kinetically significant (0.01 kcal mol^{-1} depth with respect to the second transition state). The energy surface between the two transition states would be rather flat.

For the purpose of comparison, one of the two bridging O atoms in DMP-O was replaced with S (DMP-S). The hydrolysis products are $CH_3OP(=O)(OH)(O^-)$ and CH_3S^-. As was the case in the hydrolysis of DMP-O, the solvation effects were incorporated in the calculation, and both the attacking OH^- and $-SCH_3$ were placed at the axial positions at the start of the calculation.[21] It was found that the P−S bond is cleaved in one step without any intermediate (the broken line in Figure 4).[22] The activation free energy (24.48 kcal mol^{-1}) is by 9.16 kcal mol^{-1} smaller than that in the DMP-O hydrolysis. In the transition state, the length of the P−OH(axial) bond is 2.950 Å. This bond length is significantly longer than the corresponding value in the DMP-O hydrolysis (2.125 Å). In the DMP-S hydrolysis, the P−OH bond formation is less complete in the transition state than that in the DMP-O hydrolysis. The DMP-S has a better leaving group (CH_3S^-), so that the transition state is readily formed when the attacking OH^- binds to the P atom to

(16) Kluger, R.; Colvitz, F.; Dennis, E.; Williams, D.; Westheimer, F. H. *J. Am. Chem. Soc.* **1969**, *91*, 6066−6072.
(17) Guthrie, J. P. *J. Am. Chem. Soc.* **1977**, *99*, 3991−4001.

(18) On the RHF/6-31+G* level employed in the present study, the natural population analysis gives more reasonable values of the charge than the Mulliken population analysis. Jensen, F. *Introduction to Computational Chemistry*; John Wiley & Sons: Chichester, 1999; pp 230−234.
(19) Leffler, J.; Grunwald, E. *Rates and Equilibria of Organic Reactions*; John Wiley & Sons: New York, 1963; pp 156−161.
(20) Karplus et al. pointed out that the alkaline hydrolysis of DMP-O has the early transition state, based on its Mulliken charge distribution (in ref 13).
(21) When the SCH_3 group was located at the equatorial position in the beginning of calculation, the intermediate was generated. However, it was not normally hydrolyzed but unreasonably released the SCH_3 group during the pseudo-rotation process.
(22) In a gas phase, no intermediate was formed in the alkaline hydrolysis of DMP-S.

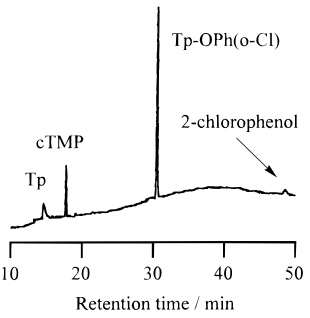

Figure 5. HPLC profile in the gradient elution for the cleavage of Tp-OPh(*o*-Cl) in 1 M NaOH (aq) at 80 °C and t = 6 h. By the intramolecular attack of the 5′-OH group, cTMP is formed. Tp is generated by the hydrolyses of both Tp-OPh-(*o*-Cl) and cTMP.[24] The gradient conditions are presented in the Experimental Section.

Table 2. Charge of Each Atom of the P−O(ester) Bond in DMP-O and of the P−S(thioester) Bond in DMP-S

	charge	
substrate	P	O or S
DMP-O	2.58	−0.89
DMP-S	2.28	−0.25

some extent. According to the natural population analysis, the extent of the formation of the P−OH(axial) bond in the transition state (α) is 20.3%, which is considerably smaller than the value (56.5%) in the DMP-O hydrolysis. The leaving group (CH_3S^-) is removed there in a greater extent (β = 66.4%). The P−OH(axial) bond and the P−SCH_3(axial) bond have similar imaginary frequencies (0.74001 and 0.53765, respectively), and both bonds are weak in the transition state. In the DMP-O hydrolysis, however, the OH^- attack must be more complete in order to remove the poorer leaving group (CH_3O^-) from the P atom. Thus, the hydrolysis rate of the Tp-OT derivatives monotonically increases with decreasing p$K_{a,lg}$ (Figure 3).

The acceleration of hydrolysis on the O→S substitution is never ascribed to the change in the electrophilicity of P atom. As shown in Table 2, the P atom of DMP−S (the charge = 2.28) is less positive than that of DMP−O (2.58). The Pauling's electronegativity of S atom (2.5) is smaller than that of O atom (3.5).[23] Accordingly, DMP-S is less susceptible to the nucleophilic attack by OH^- ion than DMP-O. The acidity of leaving group predominantly governs the reactivity of alkaline hydrolysis.

Intramolecular Attack by the 5′-OH in the Activated Tp-OT Analogues for the Transesterification. When the Tp-OT analogues having good leaving groups were incubated at pH 14, significant amounts of 3′,5′-cyclic monophosphate of thymidine (cTMP) were generated (together with the hydrolysis products). The typical HPLC profile is presented in Figure 5. Quite interestingly, Tp-OT itself did not produce cTMP at all under the same conditions. Only in these activated phosphoesters, the intramolecular attack by the 5′-OH to the P atom (path 1 in Figure 6) occurred concurrently with alkaline hydrolysis of the phosphodiester linkage (path 2). Important information on the mechanism of DNA hydrolysis is obtained by analyzing this transesterification, since the reaction mechanism is similar (nucleophilic attack by hydroxide ion vs that by alkoxide ion). Furthermore, the intramolecular reaction is much more appropriate for the analysis, since the position of the nucleophile, with respect to the P atom, is greatly restricted therein.

(1) Kinetic Studies. The rate constants for the intramolecular transesterification by the 5′-OH attack (k_{intra}) are listed in Table 1, together with the corresponding k_{hyd} values (see eqs 1 and 2 in the Experimental Section). For Tp-OPh(*p*-NO_2), Tp-OPh(*o*-Cl), and Tp-ST, the transesterification is faster than (or comparable with) the phosphodiester hydrolysis. In Tp-OCH_2CF_3, however, the transesterification is slower than the hydrolysis. With Tp-OT, the transesterification was not perceived at all and only the hydrolysis occurred.[24] Although the k_{intra} decreases with increasing p$K_{a,lg}$ as does the k_{hyd}, its dependence is far more drastic than that of k_{hyd}.

(2) Estimation of the Distance between the Nucleophile and the Electrophile for the Intramolecular Transesterification. The minimal distance between the 5′-O atom and the P-atom in Tp-OT and its analogues was evaluated by using HFMP (in Figure 2b) as a model compound. First, its structure was fully optimized by the quantum-chemical calculation. Then the C3(furanose)−OP bond and the C4(furanose)−CH_2OH bond were rotated, keeping other structural parameters unchanged. It has been found that the minimal distance between these two atoms is 2.524 Å. To shorten this distance further, enormous energy is required.

(3) Relevance between the Intramolecular Transesterification and the Phosphodiester Hydrolysis. According to the calculation on the alkaline hydrolysis of DMP-O (Figure 4), the distance between the attacking OH^- and the P atom in the transition state is 2.125 Å. It is reasonable to assume that the corresponding value in the transesterification of Tp-OT should be equal to (or smaller than) this value, since the 5′-alkoxide ion is less nucleophilic than is hydroxide ion.[14] However, the minimal distance between the 5′-O atom and the P atom in Tp-OT is 2.524 Å, as estimated above. Thus, the transesterification cannot proceed to a measurable extent. In Tp-ST hydrolysis, however, the distance between the attacking OH^- and the P in the transition state (2.950 Å) is greater than the minimal distance in the reactant. Accordingly, the transesterification efficiently takes place. The intramolecular reactions are also evident in Tp-OPh-(*p*-NO_2) and Tp-OPh(*o*-Cl),[25] whereas it is inefficient in Tp-OCH_2CF_3. The kinetic analysis and the theoretical study are completely consistent with each other.

Conclusions

By combining the kinetic studies and the theoretical studies, the mechanism of alkaline hydrolysis of DNA has

(23) *Kagaku-binran Kiso-hen*; The Chemical Society of Japan, Ed.; Maruzen: Tokyo, 1984; II-589.

(24) Considering the detection limit for cTMP, the k_{intra} value of Tp-OT is at least smaller than 3×10^{-4} h^{-1}. In this reaction, Tp and pT were formed in comparable amounts, and no cTMP was perceived. This shows that the intramolecular transesterification by the 5′-OH is not occurring. Otherwise, significant amount of cTMP should be accumulated, and, furthermore, Tp should be predominantly produced (according to control experiments, cTMP is mostly hydrolyzed to Tp under alkaline conditions).

(25) As reported previously (Borden, R. K.; Smith, M. *J. Org. Chem.* **1966**, *31*, 3247−3253), cTMP was also generated by the 3′-OH attack, when *p*-nitrophenyl ester of thymidine 5′-monophosphate was incubated at pH 14. The rate constant $k_{3'-OH} = 0.5 \times 10^{-1}$ h^{-1}. This value was significantly smaller than the k_{intra} of Tp-OPh(*p*-NO_2) (4.8×10^{-1} h^{-1}), although the k_{hyd}'s of both substrates were almost the same. The mutual conformation between the nucleophile and the target P atom is overwhelmingly important for the intramolecular transesterification.

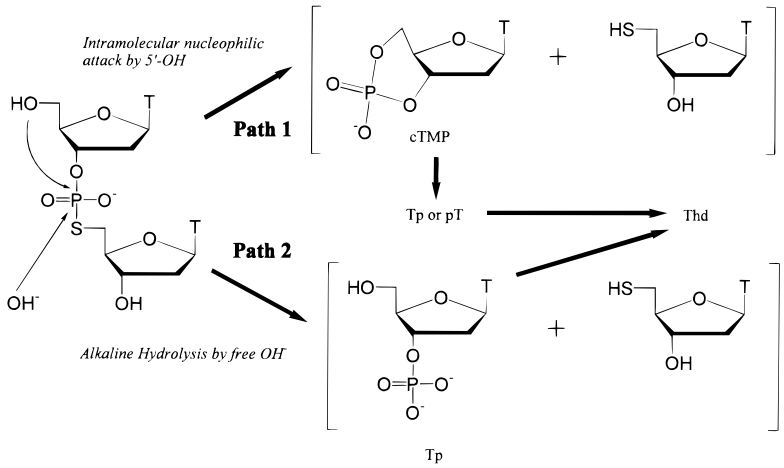

Figure 6. Two parallel reactions in the cleavage of Tp-X having good leaving groups. Path 1: the intramolecular transesterification by the 5′-OH. Path 2: alkaline hydrolysis of the phosphodiester linkage.

been clarified. It proceeds in one step without any intermediate. In the transition state, the attack by OH^- ion as a nucleophile toward the P atom is only partially complete, whereas the leaving group (alkoxide ion) is still bound to the P atom rather tightly. The lengths of the corresponding P−O bonds are 2.125 and 1.795 Å, respectively. Consistently, the slope of the Brønsted-type plot (the logarithm of hydrolysis rate vs the pK_a of leaving group) is small (−0.27). All these analyses indicate that efficient acid catalysts, which facilitate the removal of the leaving group from the P atom, are the primary requisites for prompt DNA hydrolysis under alkaline conditions. The studies on the mechanism of spontaneous and metal-catalyzed DNA hydrolysis under neutral conditions are currently under way in our laboratory.

Experimental Section

Materials. The activated Tp-OT analogues (Tp-ST, Tp-OCH_2CF_3, and Tp-OPh(*o*-Cl)) and Tp-(S)T were synthesized as described below. Pyridine was dried by KOH. Dry acetonitrile (graded for DNA synthesis) was purchased from Dojindo. The characterization of the products and reaction intermediates was made by NMR spectroscopy (^{1}H NMR at 270 MHz, ^{31}P NMR at 109.4 MHz), mass spectroscopy (TOF-MS, ESI-MS), and reversed-phase gradient HPLC equipped with an ODS column (Merck, LiChroCART 250-4, LiChrospher 100 RP-18(e)). For the TLC analysis, silica gel 60 F_{254} (Merck) was used. Tp-OT, Tp-OPh(*p*-NO_2), and cTMP were purchased from Sigma and used without further purification. Solvent water was purified by a Milli-Q Labo system (Millipore) and autoclaved. All the implements were sterilized. Great care was taken to avoid contamination by natural nucleases throughout the experiments.

(1) Synthesis of Tp-ST. In dry pyridine (5 mL), 5′-(*S*-trityl)mercapto-5′-deoxythymidine (370 mg, 0.74 mmol), synthesized as reported previously,[26] was dissolved. To this solution was added benzoyl chloride (155 mg, 1.1 mmol), and the mixture was stirred at room temperature under nitrogen for 20 h. After the reaction was quenched by water on an ice bath, the product was purified by the silica gel column chromatography (the eluent was gradually changed from CH_2Cl_2 to 5/95 EtOH/CH_2Cl_2), R_f = 0.27 (5/95 EtOH/CH_2Cl_2). The 3′-*O*-benzoyl-5′-(*S*-trityl)mercapto-5′-deoxythymidine obtained (280 mg, 0.47 mmol) was detritylated by $AgNO_3$ (160 mg, 0.94 mmol) and pyridine (86.5 mg, 1.1 mmol) in the 1:1 mixture of acetonitrile and MeOH (40 mL) at room temperature for 3 h.[27] After dithiothreitol (218 mg, 1.4 mmol) in MeOH (4 mL) was added,[27] the turbid solution was vigorously stirred for 1 h. The precipitate was filtered off, and the solvent was evaporated. The silica gel column chromatography with diethyl ether provided 3′-*O*-benzoyl-5′-mercapto-5′-deoxythymidine, R_f = 0.25 (diethyl ether).

In dry acetonitrile (2 mL), the 3′-*O*-benzoyl-5′-mercapto-5′-deoxythymidine (49.1 mg, 0.14 mmol) was treated with 5′-*O*-dimethoxytritylthymidine-3′-*O*-(2-cyanoethyl)-*N*,*N*′-diisopropylphosphoroamidite (the phosphoramidite reagent for thymidine from PerSeptive; 203 mg, 0.27 mmol) and 1*H*-tetrazole (38.1 mg, 0.54 mmol) under nitrogen for 20 min. Then, 2,6-lutidine (73.6 mg, 0.68 mmol) and *n*-tetrabutylammonium periodate in CH_2Cl_2 (2 mL) were added.[28] The fully protected Tp-ST was purified by the silica gel column chromatography, R_f = 0.44 (5/95 EtOH/AcOEt). The protecting residues were removed by the mixture of NH_4OH and MeOH (3:1) at 50 °C for 14 h and then by the deblocking solution (2% $CHCl_2COOH$ in CH_2Cl_2) for 30 min. The final product Tp-ST was extracted into water, washed by CH_2Cl_2 three times, and then purified by the reversed-phase HPLC (95/5 H_2O/acetonitrile mixture containing 50 mM ammonium formate, t_R = 61.0 min): ^{1}H NMR (D_2O) δ 7.61 (s, 1H), 7.54 (s, 1H), 6.25 (t, J = 6.6 Hz, 1H), 6.22 (t, J = 6.9 Hz, 1H), 4.85 (m, 1H), 4.44 (m, 1H), 4.20 (q, J = 3.6 Hz, 1H), 4.11 (m, 1H), 3.81 (q, ^2J = 12.4 Hz, ^3J = 3.6 Hz, 1H), 3.75 (q, ^2J = 12.5 Hz, ^3J = 4.6 Hz, 1H), 2.95−3.21 (m, 2H), 2.60 (oc, 1H), 2.31−2.44 (m, 3H), 1.86 (s, 6H); ^{31}P NMR (D_2O) δ 22.96; ESI-MS calcd for $C_{20}H_{26}N_4O_{11}PS$ [(M − H)$^-$] 561.5, found 561.4.

(2) Tp-OCH_2CF_3. 2,2,2-Trifluoroethanol (15.0 mg, 0.15 mmol) was reacted in dry acetonitrile (6 mL) with the phosphoroamidite reagent for thymidine (225 mg, 0.30 mmol) and 1*H*-tetrazole (42.0 mg, 0.60 mmol). After being kept at room temperature under nitrogen for 4 h, the mixture was treated with a 0.1 M I_2 solution of THF/2,6-lutidine/H_2O (4/1/0.1) for 30 min. The fully protected Tp-OCH_2CF_3 was purified by the silica gel column chromatography (R_f = 0.83 (2/1 AcOEt/EtOH)) and treated with the deblocking solution (4 mL) and then with NH_4OH (20 mL). The product was extracted into water and washed with CH_2Cl_2 four times. The final purification of Tp-OCH_2CF_3 was achieved by the reversed-phase HPLC (90/10 H_2O/acetonitrile mixture containing 50 mM ammonium formate, t_R = 28.9 min): ^{1}H NMR (D_2O) δ 7.64 (s, 1H), 6.31 (t, J = 6.9 Hz, 1H), 4.81 (m, 1H), 4.32 (quin, J = 8.6 Hz, 2H), 4.20 (q, J = 3.3 Hz, 1H), 3.85 (q, ^2J = 12.5 Hz, ^3J = 3.6 Hz, 1H), 3.78 (q, ^2J = 12.5 Hz, ^3J = 4.9 Hz, 1H), 2.55 (oc, 1H), 2.44 (quin, 1H), 1.89 (s, 3H); ^{31}P NMR (D_2O) δ 2.55; TOF-MS calcd for $C_{12}H_{15}F_3N_2O_8P$ [(M − H)$^-$] 403.2, found 403.6.

(26) Mag, M.; Lüking, S.; Engels, J. W. *Nucleic Acids Res.* **1991**, *19*, 1437−1441.

(27) Connolly, B.; Rider, P. *Nucleic Acids Res.* **1985**, *13*, 4485−4502.

(28) Cosstick, R.; Vyle, J. *Nucleic Acids Res.* **1990**, *18*, 829−835.

Scheme 1

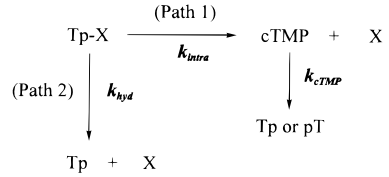

(3) Tp-OPh(*o*-Cl). In the deblocking solution (15 mL), 5′-*O*-(4,4′-dimethoxytrityl)thymidine 3′-(2-chlorophenyl)phosphate (100 mg, 0.12 mmol; from Sigma) was incubated at room temperature for 15 min. The product was purified by the reversed-phase HPLC (H_2O/acetonitrile mixture containing 50 mM ammonium formate, linear gradient from 96/4 to 60/40 at $t = 40$ min, $t_R = 29.1$ min): ^{1}H NMR (D_2O) δ 7.62 (s, 1H), 7.49 (d, $J = 7.6$ Hz, 1H), 7.37 (d, $J = 7.9$ Hz, 1H), 7.31 (t, $J = 7.3$ Hz, 1H), 7.15 (t, $J = 7.3$ Hz, 1H), 6.28 (t, $J = 7.3$ Hz, 1H), 4.90 (sep, 1H), 4.18 (q, $J = 3.6$ Hz, 1H), 3.78 (q, $^2J = 12.5$ Hz, $^3J = 3.3$ Hz, 1H), 3.71 (q, $^2J = 12.5$ Hz, $^3J = 4.9$ Hz, 1H), 2.52 (oc, 1H), 2.37 (quin, 1H), 1.86 (s, 3H).

(4) Tp-(S)T. To 3′-*O*-benzoylthymidine (17.3 mg, 0.050 mmol; from Sigma) in dry acetonitrile (2 mL) were added the phosphoroamidite reagent for thymidine (74.5 mg, 0.10 mmol) and 1*H*-tetrazole (14.0 mg, 0.20 mmol) in dry acetonitrile (1 mL each). The reaction mixture was stirred at room temperature under nitrogen for 1.5 h. Then, dry acetonitrile solution (2 mL) of tetraethylthiuram disulfide (594 mg, 2.0 mmol) was poured.[29] The mixture was incubated under nitrogen for 30 min and subjected to the silica gel column chromatography. The product ($R_f = 0.29$ (1/2 AcOEt/CH_2Cl_2)) was treated with a 3:1 mixture of NH_4OH and MeOH at 60 °C overnight and then with the deblocking solution for 15 min. The Tp-(S)T was purified by the reversed-phase HPLC (94/6 H_2O/acetonitrile mixture containing 50 mM ammonium formate, $t_R = 77.6$ min): ^{1}H NMR (D_2O) δ 7.70 (s, 1H), 7.64 (s, 1H), 6.29 (t, $J = 6.6$ Hz, 1H), 6.18 (t, $J = 6.6$ Hz, 1H), 4.94 (m, 1H), 4.56 (m, 1H), 4.08−4.21 (m, 4H), 3.84 (q, $^2J = 12.5$ Hz, $^3J = 3.3$ Hz, 1H), 3.77 (q, $^2J = 12.5$ Hz, $^3J = 4.6$ Hz, 1H), 2.53 (oc, 1H), 2.28−2.38 (m, 3H), 1.90 (s, 3H), 1.85 (s, 3H); ^{31}P NMR (D_2O) δ 60.1; ESI-MS calcd for $C_{20}H_{26}N_4O_{11}PS$ [$(M - H)^-$] 561.5, found 561.

Kinetic Analyses. Small aliquots of reaction mixtures were collected at appropriate intervals and injected to the reversed-phase HPLC after neutralization by 1 M HCl. All the products were characterized by co-injection with authentic samples under two different eluting conditions: the isocratic system (8/92 acetonitrile/water) and the linear gradient system (0/100 at $t = 0$ min → 50/50 at $t = 30$ min). The ϵ_{260} values of T-base in all the substrates and the products were determined by using authentic samples. The ϵ_{260}'s of Tp-OPh(*p*-NO_2) and Tp-OPh(*o*-Cl) were the sum of the values of those T-bases and the corresponding phenyl derivatives. With these treatments, the mass balance of each kinetic runs were satisfactory. In addition, ESI-MS and/or LC-MS were also utilized for the characterization of the products. The initial concentration of the substrate was fixed at 0.1 mM. All the pseudo-first-order rate constants presented here are the averages of the results of two or three runs.

(1) Determination of k_{hyd} and k_{intra} in Scheme 1. In the cleavage of the activated Tp-OT analogues (Tp-X), both the hydrolysis of the phosphodiester linkage and the intramolecular transesterification by the 5′-OH (formation of cTMP) concurrently proceed, as shown in Scheme 1 (see also Figures 5 and 6). The rate constant of the disappearance of Tp-X (k_{obs}) is the sum of the rate constants (k_{hyd} and k_{intra}) of these two reactions (eq 1).

$$k_{obs} = k_{hyd} + k_{intra} \quad (1)$$

On the other hand, k_{intra} can be expressed by eq 2.

$$k_{intra} = [[cTMP]_t(k_{cTMP} - k_{obs})] \times 1/[[Tp\text{-}X]_0[\exp(-k_{obs}t) - \exp(-k_{cTMP}t)]] \quad (2)$$

Here, $[cTMP]_t$ is the concentration of cTMP, which is accumulated in the reaction mixture at the reaction time t. The rate constant k_{cTMP} for alkaline hydrolysis of cTMP was determined independently by using its authentic sample. By fitting the k_{obs} and $[cTMP]_t$ values to eqs 1 and 2, k_{hyd} and k_{intra} were determined.

Quantum-Chemical Calculations. For the calculation, the Gaussian 98 program was used.[30] The geometries of all the substrates, intermediates, transition states, and products were fully optimized in the gas phase at the RHF/6-31+G* level with the frequency calculations. The Gibbs free energies were obtained by the density-functional-theory calculation with B3LYP/6-31+G* level. The solvation effects were incorporated by PCM under the recommended conditions.[31] The natural population analysis was conducted by the NBO Version 3.1.[32]

Acknowledgment. The authors should like to thank Prof. Kimitsuna Watanabe and Dr. Tsutomu Suzuki for kind assistance with the ESI-MS measurements. This work was supported by a Grant-in-Aid for Scientific Research from the Ministry of Education, Science, Sports and Culture, Japan, and JSPS Research Fellowships for Young Scientists (for N.T.).

JO000323D

(29) Zon, G.; Stec, W. J. In *Oligonucleotides and Analogues, A Practical Approach*; Eckstein, F., Ed.; Oxford University Press: New York, 1991; pp 87−108.

(30) *Gaussian 98* (Revision A.7): Frisch, M. J.; Trucks, G. W.; Schlegel, H. B.; Scuseria, G. E.; Robb, M. A.; Cheeseman, J. R.; Zakrzewski, V. G.; Montgomery, J. A.; Stratmann, R. E.; Burant, J. C.; Dapprich, S.; Millam, J. M.; Daniels, A. D.; Kudin, K. N.; Strain, M. C.; Farkas, O.; Tomasi, J.; Barone, V.; Cossi, M.; Cammi, R.; Mennucci, B.; Pomelli, C.; Adamo, C.; Clifford, S.; Ochterski, J.; Petersson, G. A.; Ayala, P. Y.; Cui, Q.; Morokuma, K.; Malick, D. K.; Rabuck, A. D.; Raghavachari, K.; Foresman, J. B.; Cioslowski, J.; Ortiz, J. V.; Baboul, A. G.; Stefanov, B. B.; Liu, G.; Liashenko, A.; Piskorz, P.; Komaromi, I.; Gomperts, R.; Martin, R. L.; Fox, D. J.; Keith, T.; Al-Laham, M. A.; Peng, C. Y.; Nanayakkara, A.; Gonzalez, C.; Challacombe, M.; Gill, P. M. W.; Johnson, B. G.; Chen, W.; Wong, M. W.; Andres, J. L.; Gonzalez, C.; Head-Gordon, M.; Replogle, E. S.; Pople, J. A. Gaussian, Inc., Pittsburgh, PA, 1998.

(31) Solvent, water; Model, PCM/UAHF; Icomp = 4; Version, Matrix inversion; Cavity, Pentakisdodecahedra with 60 initial tesserae. Barone, V.; Cossi, M.; Tomasi, J. *Chem. Phys.* **1997**, *107*, 3210−3221.

(32) NBO Version 3.1, Glendening, E. D.; Reed, A. E.; Carpenter, J. E.; Weinhold, F.